International Journal of Modern Physics B
Vol. 24, No. 27 (2010) 5371–5378

DOI: 10.1142/S0217979210055925

World Scientific
www.worldscientific.com

CURRENT CONDUCTION MECHANISMS OF ATOMIC-LAYER-DEPOSITED Al_2O_3/NITRIDED SiO_2 STACKING GATE OXIDE ON 4H-SiC

K. Y. CHEONG*, Z. LOCKMAN and A. AZIZ

School of Materials and Mineral Resources Engineering, Universiti Sains Malaysia, Engineering Campus, 14300 Nibong Tebal, Seberang Perai Selatan, Penang, Malaysia
** cheong@eng.usm.my*

J. H. MOON and H. J. KIM

Department of Materials Science and Engineering, Seoul National University, Seoul 151-742, Korea

W. BAHNG and N.-K. KIM

Integrated Power Supply Research Group, Advanced Materials & Application Research Division, Korea Electrotechnology Research Institute, 70 Boolmosangil, Changwon, 641-120, Korea

Z. HASSAN

School of Physics, Universiti Sains Malaysia, 11800 Penang, Malaysia

Received 7 July 2008

Current conduction mechanisms of atomic-layer deposited Al_2O_3 (13 nm) stacked on different thermal nitrided SiO_2 thicknesses (2, 4, and 6 nm) on n-type 4H-SiC have been systematically analyzed. It has been observed that the oxides were thermally stable at the investigated temperature range (25–140°C). By using different conduction process models, such as Schottky emission, direct tunneling, Fowler–Nordheim tunneling, Poole–Frenkel emission, and space-charge limited conduction, which consists of three limited conduction processes, namely, Ohm's law, Child's law, and trap-filled limit, the conduction mechanisms of charge through the oxides have been evaluated. It has been found that the conduction mechanisms were not affected by the investigated temperature range. A relationship plot has been proposed among nitrided SiO_2 thickness, electric field, and conduction mechanisms.

Keywords: Fowler–Nordheim tunneling; Poole–Frenkel emission; Ohm's law; Electric breakdown field.

1. Introduction

The superb electrical, physical, and chemical properties of silicon carbide (SiC) have promoted it to be used as the substrate for high power metal-oxide-semiconductor (MOS) based devices.[1] Typically, thermal nitrided SiO_2 has been employed as the gate oxide of the device owing to its low SiC–SiO_2 interface and near interface trap density, high reliability, and good thermal stability.[2–7] Due to its relatively low dielectric constant value ($k = 3.9$) compared to SiC ($k_{SiC} = 9.7$), approximately 2.5 times higher vertical electric field (E) is being imposed on the oxide compared to the substrate. Hence, the oxide may be pre-maturely broken down. In order to resolve this issue, high-k gate oxides have been extensively studied. This is because E is scaled by a factor of k_{SiC}/k, as a result, smaller vertical electric field strength can be imposed onto the oxide.[1]

Of numerous high-k materials,[8–14] Al_2O_3 has been investigated due to its high-k value ($k = 8.3$), good thermal stability, and compatibility to SiC. These properties may change according to the oxide deposition techniques.[9,13,14] Recently, positive results have been demonstrated by atomic-layer deposited Al_2O_3 on 6H and 4H-SiC, but its leakage current is still considered high.[12] This is attributed to the low conduction band offset between the oxide and semiconductor ($\Delta E_C = 1.5$ eV).[14] In order to increase the band offset, a thin buffer layer of nitrided SiO_2 has been sandwiched in between Al_2O_3 and SiC.[9,12,14] With this structure, a significant improvement in leakage current and oxide breakdown field (E_{BD}) of the MOS structure has been reported. These improvements are attributed to the way current conducts through the oxide. The current-conduction mechanisms of Al_2O_3/4H-SiC system have been reported recently, but the mechanisms of Al_2O_3/SiO_2/4H-SiC stacking structure have yet to be reported.[9] Therefore, it is the aim of this letter to report the current-conduction mechanisms of atomic-layer deposited Al_2O_3 (13 nm) stacked on various thickness of thermally nitrided SiO_2 (2, 4, and 6 nm) based on n-type 4H-SiC.

2. Experimental Method

Pre-cleaned n-type 4H-SiC wafers and 8° off (0001) oriented with 10-μm thick epilayer doped with $(1 - 4) \times 10^{16}$ cm^{-3} of nitrogen were used to fabricate the MOS-capacitor test structures. Thermal-nitrided SiO_2 was grown on SiC in 10% N_2O–90% N_2 ambient at 1175°C for a certain period so that a 2-, 4-, and 6-nm thick oxide is achieved. After the oxide growth, the samples were cooled down to 800°C in high-purity N_2 gas flow. Then, they were transferred to an atomic-layer-deposition system whereby a 13-nm thick Al_2O_3 was simultaneously deposited onto the samples. The atomic-layer-deposition procedure has been described elsewhere.[15] After that, a layer of nickel was sputtered on the oxides to form gate electrodes. The subsequent MOS-capacitor fabrication process has been described elsewhere.[4] A *Semiconductor Parameter Analyzer* (HP-4156) was used to measure leakage current of the MOS capacitor with an area, A, of 1.30×10^{-3} cm^2 at various temperatures

(25–140°C). The gate current (I_G) as a function of forward gate-voltage sweep, V_G, (ramping rate = 0.3 V/s) was recorded. The parameters I_G and V_G were also transformed into current density (J) and electric field (E) using the following expressions:

$$J = I_G/A \tag{1}$$

$$E = (V_G - V_{FB})/t_{ox} \tag{2}$$

where V_{FB} and t_{ox} are the flat band voltage and oxide thickness. The results of MOS characteristics as a function of nitrided-SiO_2 thickness have been reported earlier.[12]

3. Results and Discussion

The J–E measurements of the investigated stacking gate oxides at various temperatures (25–140°C) have been presented in Ref. 12. From these results, conduction mechanisms through these oxides have been systematically evaluated using different conduction models, such as Schottky emission, direct tunneling, Fowler–Nordheim (FN) tunneling, Poole–Frenkel (PF) emission, and space-charge limited conduction, which consists of three limited conduction processes, namely, Ohm's law, Child's law, and trap-filled limit. In the evaluation, effect of temperature has been taken into consideration when linear fitting is being performed.

Figure 1 shows a typical plot of J–V_G measured at room temperature for the three investigated oxides. At low electric field, current conduction obeys Ohm's law, which is revealed by the filled symbols in the figure. Ohm's law can be

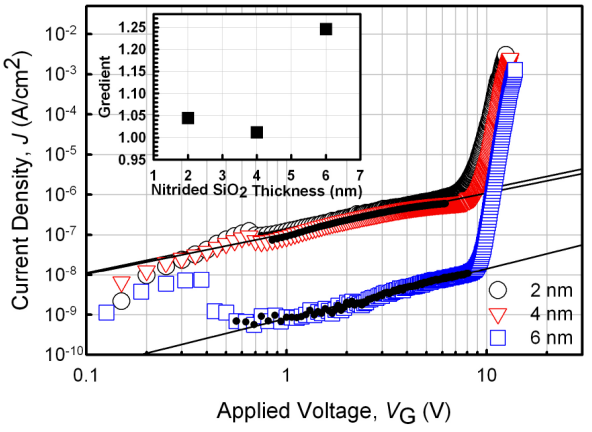

Fig. 1. Current density, J, as a function of applied gate voltage, V_G, at room temperature for $Ni/Al_2O_3/SiO_2/4H\text{-}SiC$ MOS capacitors with different thickness (2, 4, and 6 nm) of nitrided SiO_2 (open symbols). The plots are fitted linearly with Ohm's law (filled symbols) and the gradients of each plot extracted from various temperatures (25–140°C) are presented in the inset of the figure.

mathematically described as follows[9]:

$$J_{\mathrm{Ohm}} = qn_0\mu\frac{V_{\mathrm{G}}}{t_{ox}} \tag{3}$$

where, J_{Ohm}, q, n_0, and μ, are current density due to Ohm's law, electronic charge, concentration of free charge carrier in thermal equilibrium, and electronic mobility in the oxide.

Current conduction via this mechanism is attributed to the thermal excitation of trapped electrons from bulk oxides of both Al_2O_3 and SiO_2 when an electric field is applied. The density of these excited electrons is much higher than that injected from the SiC substrate [path (1) in Fig. 2]. The gradient of the linear fitted region for the respective oxides are presented in the inset of Fig. 1. The gradient of the oxides obtained from higher temperature is the same as those measured at room temperature. Ideally, current conduction obeying Ohm's law should reveal a gradient of unity and it has been demonstrated by stacking oxides with 2- and 4-nm thick nitrided SiO_2 but a small deviation to a higher value has been shown

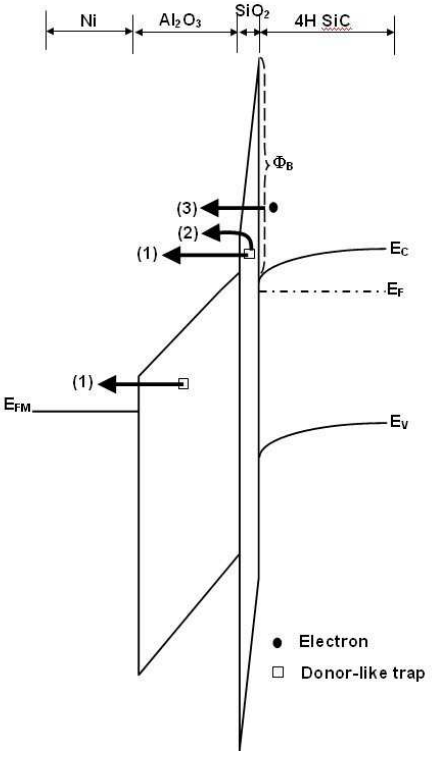

Fig. 2. Energy-band diagram of MOS structures with Al_2O_3 stacked on SiO_2 gates. The numbering (1) to (3) refers to respective leakage paths due to Ohm's law, Poole–Frenkel emission, and Fowler–Nordheim tunnelling, respectively. E_{C}, E_{F}, E_{V}, E_{FM}, and Φ_{B} are the conduction band edge, Fermi level, valence band edge, Fermi level of Ni, and effective barrier height, respectively.

in stacking oxide with 6-nm thick nitrided SiO_2. Only Ohm's law is governing the current conduction process at this low electric field region ($\sim 0.2 - 4.2$ MV/cm, depending on the SiO_2 thickness) for the three stacking oxides. This is rather similar to those current conducting through nitrided SiO_2/4H-SiC structure.[3] However, for Al_2O_3/4H-SiC structure, trap-filled limit and Poole–Frenkel (PF) emission are the dominant mechanisms for current conduction at the same electric field region.[9]

As the electric field is increasing (5.7–7.4 MV/cm), PF emission has been identified as the governing mechanism for current conducting through stacking oxide with 2-nm thick nitrided SiO_2 (Fig. 3). This mechanism is a bulk-limited conduction and can be described as[9]:

$$J = (qN_c\mu)E\exp\{[-q(\phi_t - \sqrt{qE/\pi\varepsilon_r\varepsilon_0})]/[KT]\} \tag{4}$$

where N_c, ε_r, ϕ_t, and K are the density of states in the conduction band, dynamic dielectric constant, trap energy level, and Boltzmann's constant, respectively. From the gradient of the linearity, ε_r has been extracted and the values range from 4.78 to 5.08, depending on the measured temperature. This value is lower than the dielectric constant (6.9) obtained from high-frequency capacitance-voltage measurement.[12] PF emission is due to field-enhanced thermal excitation of trapped electron into the conduction band [path (2), Fig. 2] and it may be originated from bulk Al_2O_3 and not from bulk nitrided SiO_2. This is because, based on current conduction of Al_2O_3/4H–SiC structure,[9] it has shown a similar emission process at the investigated electric-field range.

In addition to PF emission, FN tunneling through the stacking oxide with 2-nm thick nitrided SiO_2 can also be well-fitted [path (3), Fig. 2]. Therefore, it is unable to differentiate which mechanism dominates the conduction. The FN tunneling is also being revealed in other stacking oxides. The FN plots of the three investigated

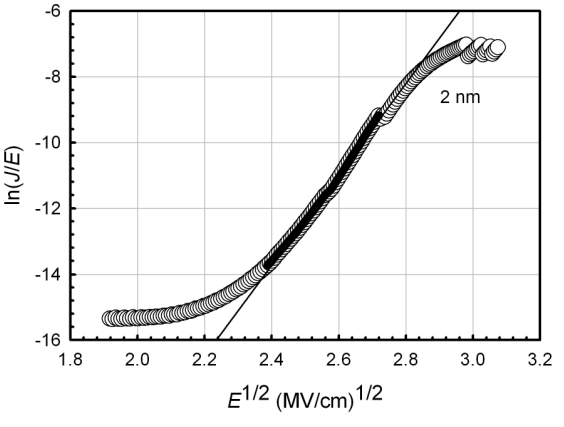

Fig. 3. A typical room temperature Pool–Frenkel (PF) emission plot [$\ln(J/E)$ versus $E^{1/2}$] measured from Ni/Al_2O_3/SiO_2/4H–SiC MOS capacitor with 2-nm thick nitrided SiO_2 (open symbol). Gradient of the linearly fitted region (filled symbol) is used to calculate dynamic dielectric constant, ε_r, of the stacked gate oxide.

stacking oxides are presented in Fig. 4. From the FN plots, effective barrier height, Φ_B, between conduction band edge of SiC and nitrided SiO_2 have been extracted and is shown in the inset of the figure. The Φ_B is increasing with the increase of nitrided SiO_2 thickness. The thickest nitrided SiO_2 has shown the Φ_B value of 2.70 eV, which is closer to its theoretical value. This indicates that the effect of nitrided SiO_2 becomes dominant as the thickness increases. When these oxides are investigated at higher temperature, there is no obvious change in the Φ_B value; suggesting that these stacking oxides are thermally stable within the investigated

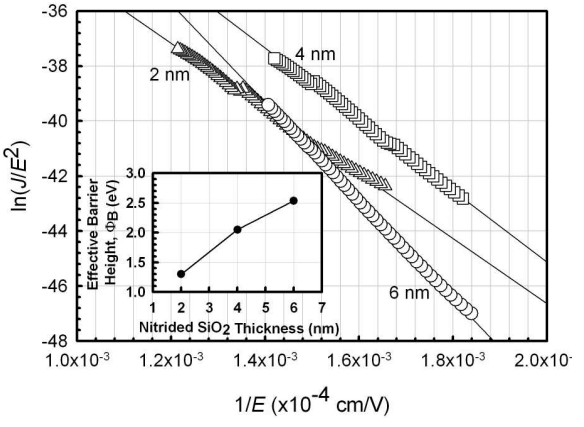

Fig. 4. Typical Fowler–Nordheim (FN) tunneling plots as a function of nitrided SiO_2 thickness for the investigated $Ni/Al_2O_3/SiO_2/4H$–SiC MOS capacitors. Effective barrier height, Φ_B, of the respective samples (inset of the figure) have been extracted and calculated from the gradient of linear fitted region from various temperatures (25–140° C) FN plots.

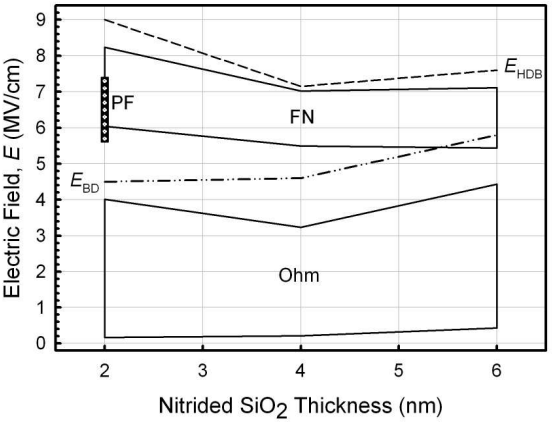

Fig. 5. A relationship among nitridied SiO_2 thickness, electric field, and current conduction mechanism through atomic-layer deposited Al_2O_3/thermal nitrided SiO_2 gate on n-type 4H–SiC. The abbreviations FN, PF, Ohm, E_{HDB}, and E_{BD} represent Fowler–Nordheim tunneling, Poole–Frenkel emission, Ohm's law conduction, hard oxide breakdown, and oxide breakdown.

temperature range. Figure 5 presents current-conduction mechanisms of the three investigated stacking oxides as a function of nitrided SiO_2 thickness and E obtained at room temperature. Depending on the nitrided-oxide thickness (approximately in between 4 to 5.5 MV/cm,), there is still some region with unknown mechanism. Besides the conduction mechanisms, hard oxide breakdown field (E_{HBD}) and oxide breakdown field (E_{BD}) are included. E_{HBD} is defined as any electric field that induces an instantaneous increase of current density while E_{BD} is associated with any electric field that could cause leakage current density higher than 10^{-6} A/cm^2. Based on this figure, mechanism responsible for current conduction through the stacking oxides as a function of nitrided SiO_2 thickness can be identified.

4. Conclusion

The current conduction mechanisms of atomic-layer deposited Al_2O_3 (13 nm)/ thermal nitrided SiO_2 gates stacked on n-type 4H-SiC have been systematically investigated. The effect of nitrided SiO_2 thickness (2, 4, and 6 nm) on the stacking gate has been studied. It has been found that the oxides were thermally stable and the conduction mechanisms were independent on temperature (25–140°C). Several mechanisms have been identified, which are responsible for current conduction through the investigated oxides, depending on the nitrided SiO_2 thickness. The relationships among the oxide thickness, electric field, and conduction mechanisms have been established.

Acknowledgments

One of the authors (KYC) would like to acknowledge the financial support of this work from the Higher Education Minister of Malaysia (MOHE) through Fundamental Research Grant Scheme (FRGS) (Grant number: 6070025).

References

1. Agarwal, S.-H. Ryu and J. Palmour, Power MOSFETs, in *4H-SiC: Device Design and Technology, in Recent Major Advances in SiC*, eds. W. J. Choyke, H. Matsunami and G. Pensl (Springer, Berlin, 2004), pp. 785–812.
2. K. Y. Cheong, S. Dimitrijev and J. Han, *J. Appl. Phys.* **93**, 5682 (2003).
3. K. Y. Cheong, W. Bahng and N.-K. Kim, *Phys. Letts. A* **372**, 529 (2008).
4. K. Y. Cheong, W. Bahng and N.-K. Kim, *Microelectron. Eng.* **83**, 65 (2006).
5. K. Y. Cheong, W. Bahng and N.-K. Kim, *Appl. Phys. Letts.* **87**, 212102 (2005).
6. K. Y. Cheong, S. Dimitrijev and J. Han, *IEEE Trans. Electron Dev.* **51**, 1361 (2004).
7. J. P. Xu, P. T. Lai, C. L. Chan, B. Li and Y. C. Cheng, *IEEE Electron Dev. Letts.* **21**, 298 (2000).
8. K. Y. Cheong, J. H. Moon, T. J. Park, J. H. Kim, C. S. Hwang, H. J. Kim, W. Bahng and N.-K. Kim, *IEEE Trans. Electron Dev.* **54**, 3409 (2007).
9. K. Y. Cheong, J. H. Moon, H. Kim, W. Bahng and N. K. Kim, *Appl. Phys. Letts.* **90**, 162113 (2007).
10. L. A. Lipkin and J. Palmour, *IEEE Trans. Electron Dev.* **46**, 525 (1999).

11. J. H. Moon, D. I. Eom, S. Y. No, H. K. Song, J. H. Yim, H. J. Na, J. B. Lee and H. J. Kim, *Mater. Sci. Forum* **527–529**, 1083 (2006).
12. K. Y. Cheong, J. H. Moon, D. Eom, H. J. Kim, W. Bahng and N.-K. Kim, *Electrochem. Solid-State Letts.* **10**, H69 (2007).
13. S. W. Huang and J. G. Hwu, *IEEE Trans. Electron Dev.* **51**, 1877 (2004).
14. V. V. Afanas'ev, A. Stesmans, F. Chen, S. A. Campbell and R. Smith, *Appl. Phys. Letts.* **82**, 922 (2003).
15. S. Y. No, D. Eom, C. S. Hwang and H. J. Kim, *J. Electrochem. Soc.* **153**, F87 (2006).